Integral Equation Solution to the Guidance and Leakage Properties of Coupled Dielectric Strip Waveguides

JEAN-FU KIANG, SAMI M. ALI, SENIOR MEMBER, IEEE, AND JIN AU KONG, FELLOW, IEEE

Abstract—**The guidance and leakage properties of single and coupled dielectric strip waveguides are analyzed using the dyadic Green's function and integral equation formulation. Galerkin's method is used to solve the integral equation for the dispersion relation. The effects of the geometrical and the electrical parameters on the dispersion relation are investigated. A method to predict the occurrence of leakage is proposed. The properties of the even and the odd leaky modes are also investigated. Results are compared with previous analysis and shown to be in good agreement.**

I. INTRODUCTION

THE LEAKAGE phenomenon is important in the area of millimeter-wave integrated circuits and integrated optics. Theoretical analyses and experiments have been performed to investigate this phenomenon [1]–[6]. The leakage is due to the TE–TM coupling occurring at the geometrical discontinuities, and the leaky power in the form of a surface wave propagates in the background medium. The leakage loss can be larger than the dielectric loss for some low-loss materials and may cause crosstalk to neighboring circuit components. On the other hand, the leakage properties can be deliberately utilized in designing directional couplers.

There are several methods used to analyze dielectric strip waveguides. The approximate field matching method [7] is used to analyze the rectangular dielectric waveguide. This method considers only the fields in the regions attached to the four sides of the guide cross section, and the fields in the other regions are assumed negligible. The transverse propagation constants are determined by solving the corresponding slab waveguide problems in two transverse directions of the guide cross section separately. This method is an approximate one, and can only predict the real part of the propagation constant.

Manuscript received April 5, 1989; revised September 5, 1989. This work was supported by the Joint Services Electronics Program under Contract DAAL03-89-C-0001, by RADC Contract F19628-88-K-0013, by NSF Grant 8620029-ECS, by ARO Contract DAAL03-88-J-0057, and by ONR Contract N00014-89-J-1019.

J.-F. Kiang was with the Department of Electrical Engineering and Computer Science, Massachusetts Institute of Technology, Cambridge, MA 02139. He is now with the IBM Thomas J. Watson Research Center, Yorktown Heights, NY 10598.

S. M. Ali and J. A. Kong are with the Department of Electrical Engineering and Computer Science and Research Laboratory of Electronics, Massachusetts Institute of Technology, Cambridge, MA 02139.

IEEE Log Number 8932003.

The effective dielectric constant (EDC) method [8] has been used to solve for the dispersion relations of dielectric strip waveguides consisting of more than two constituent regions in the cross section. This method is applied when the width of each constituent region is large compared with the thickness of the guiding layers, and the difference of the effective dielectric constants between different constituent regions is small. However, the EDC method neglects the geometrical discontinuities across the interfaces between constituent regions and cannot be used to predict the imaginary part of the propagation constant; thus the leakage is not considered.

The mode-matching technique has been used to solve for the propagation constant of dielectric strip waveguides [9]. Using this method, the leakage properties of the guiding structure has been investigated [1]–[3], [10]. This technique can be applied to guiding structures in which the modes of the constituent regions can be determined. However, it cannot be applied when the cross section of the guiding structure is of arbitrary shape or has inhomogeneous dielectric constant.

The finite element method [11], [12] and the finite difference method [13] have been used to solve for the dispersion characteristics of the dielectric waveguides. However, the leakage effect was not investigated.

The integral equation method has been used to solve for the dispersion relation of the rectangular dielectric waveguide [14]. This method incorporates the continuous spectrum, and hence the radiation loss is taken into account. However, no results concerning practical single and coupled dielectric strip waveguides were presented; and the leakage phenomenon was not investigated.

In this paper, an integral equation formulation using the dyadic Green's function [15], [16] is derived to solve for the dispersion relation of single and coupled dielectric strip waveguides. A method to predict the leakage is presented, and the leakage properties are investigated. In Section II, the integral equation formulation for an arbitrary number of inhomogeneous dielectric strips is derived; in Section III, Galerkin's method is used to obtain the matrix eigenvalue equations. Numerical results and discussions are presented in Section IV.

0018-9480/90/0200-0193$01.00

II. Integral Equation Formulation

In Fig. 1, there are N inhomogeneous dielectric strips of arbitrary cross section embedded in layer (l) of a planar stratified medium. The whole structure is assumed to be uniform along the propagation direction y. Assume that the permittivity of the dielectric strips is $\epsilon(\boldsymbol{r})$, then the electric field in layer (l) can be represented by the dyadic Green's function and the equivalent polarization current in the dielectric strips as

$$\boldsymbol{E}(\boldsymbol{r}) = i\omega\mu_0 \int\int\int_V dV' \bar{\bar{G}}_{ll}(\boldsymbol{r},\boldsymbol{r}')\cdot\boldsymbol{J}_{eq}(\boldsymbol{r}')$$

$$= \omega^2\mu_0 \int\int\int_V dV' \bar{\bar{G}}_{ll}(\boldsymbol{r},\boldsymbol{r})\cdot\delta\epsilon(\boldsymbol{r}')\boldsymbol{E}(\boldsymbol{r}') \quad (1)$$

where $\boldsymbol{J}_{eq}(\boldsymbol{r}) = -i\omega\delta\epsilon(\boldsymbol{r})\boldsymbol{E}(\boldsymbol{r})$, $\delta\epsilon(\boldsymbol{r}) = \epsilon(\boldsymbol{r}) - \epsilon_l$, and V is the space occupied by the dielectric strips. The dyadic Green's function $\bar{\bar{G}}_{ll}(\boldsymbol{r},\boldsymbol{r}')$ can be represented in the spectral domain as

$$\bar{\bar{G}}_{ll}(\boldsymbol{r},\boldsymbol{r}') = \frac{i}{8\pi^2}\int\int_{-\infty}^{\infty} d\boldsymbol{k}_s e^{i\boldsymbol{k}_s\cdot(\boldsymbol{r}_s-\boldsymbol{r}_s')}\bar{\bar{g}}_{ll}(\boldsymbol{k}_s,z,z') - \frac{\hat{z}\hat{z}}{k_l^2}\delta(\boldsymbol{r}-\boldsymbol{r}') \quad (2)$$

where

$$\boldsymbol{k}_s = \hat{x}k_x + \hat{y}k_y$$

$$\boldsymbol{r}_s = \hat{x}x + \hat{y}y$$

$$\boldsymbol{r}_s' = \hat{x}x' + \hat{y}y'$$

and $\bar{g}_{ll}(\boldsymbol{k}_s, z, z')$ is the Fourier transform of the principal value part of $\bar{\bar{G}}_{ll}(\boldsymbol{r},\boldsymbol{r}')$ with respect to $\boldsymbol{r}_s$. The first term on the right-hand side of (2) is the principal value part of the dyadic Green's function, and the second term is the source dyadic.

For $z > z'$, the explicit form of $\bar{\bar{g}}_{ll}(\boldsymbol{k}_s, z, z')$ is given by [15], [16]

$$\bar{\bar{g}}_{ll}(\boldsymbol{k}_s, z_>, z_<')$$

$$= \frac{1}{k_{lz}\left(1 - R^{\mathrm{TE}}_{\cup l}R^{\mathrm{TE}}_{\cap l}e^{2ik_{lz}h_l}\right)}\cdot\left[\hat{h}(k_{lz})e^{ik_{lz}z_l} + R^{\mathrm{TE}}_{\cup l}\hat{h}(-k_{lz})e^{ik_{lz}(2h_l - z_l)}\right]\cdot\left[\hat{h}(k_{lz})e^{-ik_{lz}z_l'} + R^{\mathrm{TE}}_{\cap l}\hat{h}(-k_{lz})e^{ik_{lz}z_l'}\right]$$

$$+ \frac{1}{k_{lz}\left(1 - R^{\mathrm{TM}}_{\cup l}R^{\mathrm{TM}}_{\cap l}e^{2ik_{lz}h_l}\right)}\cdot\left[\hat{v}(k_{lz})e^{ik_{lz}z_1} + R^{\mathrm{TM}}_{\cup l}\hat{v}(-k_{lz})e^{ik_{lz}(2h_l - z_l)}\right]\cdot\left[\hat{v}(k_{lz})e^{-ik_{lz}z_l'} + R^{\mathrm{TM}}_{\cap l}\hat{v}(-k_{lz})e^{ik_{lz}z_l'}\right] \quad (3a)$$

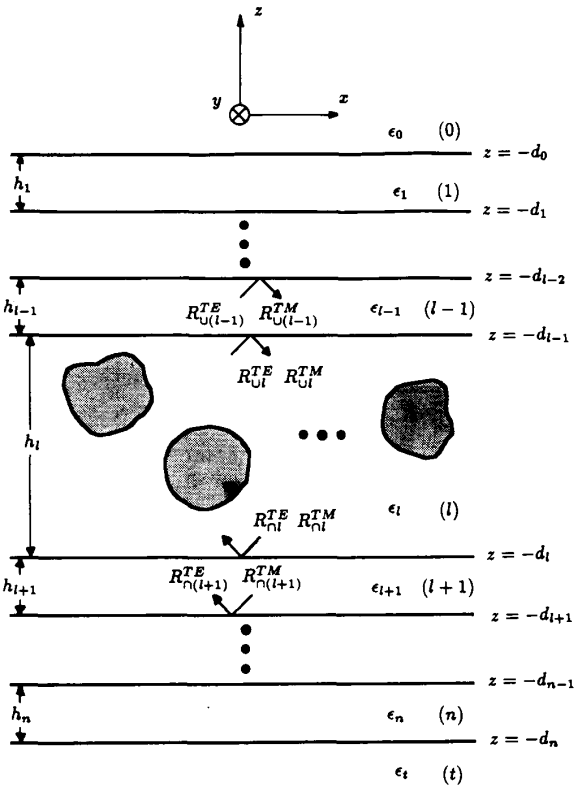

Fig. 1. Geometrical configuration of N dielectric strips embedded in layer (l) of a planar stratified medium.

and for $z < z'$, we have

$$\bar{g}_{ll}(\boldsymbol{k}_s, z_<, z_>')$$

$$= \frac{1}{k_{lz}\left(1 - R^{\mathrm{TE}}_{\cup l}R^{\mathrm{TE}}_{\cap l}e^{2ik_{lz}h_l}\right)}\cdot\left[\hat{h}(-k_{lz})e^{-ik_{lz}z_l} + R^{\mathrm{TE}}_{\cap l}\hat{h}(k_{lz})e^{ik_{lz}z_l}\right]\cdot\left[\hat{h}(-k_{lz})e^{ik_{lz}z_l'} + R^{\mathrm{TE}}_{\cup l}\hat{h}(k_{lz})e^{ik_{lz}(2h_l - z_l')}\right]$$

$$+ \frac{1}{k_{lz}\left(1 - R^{\mathrm{TM}}_{\cup l}R^{\mathrm{TM}}_{\cap l}e^{2ik_{lz}h_l}\right)}\cdot\left[\hat{v}(-k_{lz})e^{-ik_{lz}z_l} + R^{\mathrm{TM}}_{\cap l}\hat{v}(k_{lz})e^{ik_{lz}z_l}\right]\cdot\left[\hat{v}(-k_{lz})e^{ik_{lz}z_l'} + R^{\mathrm{TM}}_{\cup l}\hat{v}(k_{lz})e^{ik_{lz}(2h_l - z_l')}\right] \quad (3b)$$

here z_l and z_l' are the local coordinates defined as $z_l = z + d_l$, $z_l' = z' + d_l$, and

$$\hat{h}(\pm k_{lz}) = \frac{\hat{x}k_y - \hat{y}k_x}{k_s}$$

$$\hat{v}(\pm k_{lz}) = \mp\frac{k_{lz}\bar{k}_s}{k_l k_s} + \hat{z}\frac{k_s}{k_l} \quad (4)$$

where $k_s = |\boldsymbol{k}_s|$ and $k_{lz} = k_l^2 - k_s^2$ with $\mathrm{Im}(k_{lz}) \geq 0$.

In (3), $R^{TM}_{\cup l}$ and $R^{TE}_{\cup l}$ are the reflection coefficients of the TM and the TE modes at the upper boundary of layer (l), $R^{TM}_{\cap l}$ and $R^{TE}_{\cap l}$ are the reflection coefficients of the TM and the TE modes at the lower boundary of layer (l). They can be obtained recursively as

$$R^{\alpha}_{\cup l} = \frac{R^{\alpha}_{l(l-1)} + R^{\alpha}_{\cup(l-1)} e^{2ik_{(l-1)z}h_{l-1}}}{1 + R^{\alpha}_{l(l-1)} R^{\alpha}_{\cup(l-1)} e^{2ik_{(l-1)z}h_{l-1}}}, \qquad \alpha = (\mathrm{TE}, \mathrm{TM}) \tag{5a}$$

$$R^{\alpha}_{\cap l} = \frac{R^{\alpha}_{l(l+1)} + R^{\alpha}_{\cap(l+1)} e^{2ik_{(l+1)z}h_{l+1}}}{1 + R^{\alpha}_{l(l+1)} R^{\alpha}_{\cap(l+1)} e^{2ik_{(l+1)z}h_{l+1}}}, \qquad \alpha = (\mathrm{TE}, \mathrm{TM}) \tag{5b}$$

where $R^{\alpha}_{l(l-1)}$ and $R^{\alpha}_{l(l+1)}$ are the Fresnel reflection coefficients of the α mode across the interfaces at $z = -d_{l-1}$ and $z = -d_l$, respectively. The explicit forms are

$$R^{TE}_{l(l\pm1)} = \frac{k_{lz} - k_{(l\pm1)z}}{k_{lz} + k_{(l\pm1)z}} \qquad R^{TM}_{l(l\pm1)} = \frac{\epsilon_{l\pm1} k_{lz} - \epsilon_l k_{(l\pm1)z}}{\epsilon_{l\pm1} k_{lz} + \epsilon_l k_{(l\pm1)z}}. \tag{6}$$

Substituting the dyadic Green's function in (2) into (1), we obtain

$$\boldsymbol{E}(\boldsymbol{r}) + \frac{\delta\epsilon(\boldsymbol{r})}{\epsilon_l}\hat{z}E_z(\boldsymbol{r}) = \frac{i\omega^2\mu_0}{8\pi^2}\int\int\int_V dV' \cdot \int\int_{-\infty}^{\infty} d\boldsymbol{k}_s e^{i\boldsymbol{k}_s\cdot(\boldsymbol{r}_s - \boldsymbol{r}_s')}\delta\epsilon(\boldsymbol{r}')\bar{\bar{g}}_{ll}(\boldsymbol{k}_s, z, z')\cdot\boldsymbol{E}(\boldsymbol{r}') \tag{7}$$

where the source dyadic contribution has been collected to be the second term on the left-hand side. If the observation point is outside of the source region, this term vanishes automatically.

We assume that the pth eigenmode can be represented as $\boldsymbol{E}_p(\boldsymbol{\rho})e^{i\eta y}$, where η is the propagation constant along the y direction, and $\boldsymbol{\rho} = \hat{x}x + \hat{z}z$. Equation (7) can thus be reduced to

$$\boldsymbol{E}_p(\boldsymbol{\rho}) + \frac{\delta\epsilon(\boldsymbol{\rho})}{\epsilon_l}\hat{z}E_{pz}(\boldsymbol{\rho}) = \frac{i\omega^2\mu_0}{4\pi}\int\int_S d\boldsymbol{\rho}'\delta\epsilon(\boldsymbol{\rho}') \cdot \int_{-\infty}^{\infty} dk_x e^{ik_x(x-x')}\bar{\bar{g}}_{ll}(k_x, \eta, z, z')\cdot\boldsymbol{E}_p(\boldsymbol{\rho}') \tag{8}$$

where S is the cross section of the guiding regions where $\delta\epsilon(\boldsymbol{\rho}) = \epsilon(\boldsymbol{\rho}) - \epsilon_1 \neq 0$.

Consider two identical dielectric strips embedded in layer (l) and located symmetrically with respect to $x = 0$. The separation s between the two strips is defined as the shortest distance between them. For this symmetrical configuration, both the even and the odd mode exist. We denote the even (odd) mode as a mode with E_z an even (odd) function, and H_z an odd (even) function of x. A magnetic (electric) wall can be put at $x = 0$ without affecting the field distributions.

The coupled integral equation can be written as

$$\begin{aligned}\boldsymbol{E}_p(\boldsymbol{\rho}) + \frac{\delta\epsilon(\boldsymbol{\rho})}{\epsilon_l}\hat{z}E_{pz}(\boldsymbol{\rho}) &= \frac{i\omega^2\mu_0}{4\pi}\int\int_{S_1} d\boldsymbol{\rho}'\delta\epsilon(\boldsymbol{\rho}')\int_{-\infty}^{\infty} dk_x e^{ik_x(x-x')}\bar{\bar{g}}_{ll}(k_x, \eta, z, z') \cdot \boldsymbol{E}_p(\boldsymbol{\rho}') \\ &+ \frac{i\omega^2\mu_0}{4\pi}\int\int_{S_2} d\boldsymbol{\rho}'\delta\epsilon(\boldsymbol{\rho}')\int_{-\infty}^{\infty} dk_x e^{ik_x(x-x')}\bar{\bar{g}}_{ll}(k_x, \eta, z, z') \cdot \boldsymbol{E}_p(\boldsymbol{\rho}'), \qquad \boldsymbol{\rho} \text{ on } S_1 \text{ or } S_2\end{aligned} \tag{9}$$

where S_1 and S_2 are the cross sections of the dielectric strips. The source dyadic contribution has been collected as the second term on the left-hand side of (9). On the right-hand side of (9), the first (second) integral represents the contribution by the equivalent polarization current in the first (second) dielectric strip.

In the next section, Galerkin's method is used to solve the integral equations (8) and (9) for the dispersion relation $\eta(\omega)$.

III. Numerical Solution

For practical applications, the cross section of the dielectric strips can be assumed to have a rectangular shape. For a single dielectric strip of width w and thickness $t_g = t_{\mathrm{I}} - t_{\mathrm{II}}$ as shown in Fig. 2, we divide the cross section S into N by M cells of equal area. The length of each cell is $D_x = w/N$ along the x direction, and $D_z = t_g/M$ along with z direction. The center coordinate of the (n, m) cell, S_{nm}, is denoted by (x_n, z_m) with $1 \leqslant n \leqslant N$ and $1 \leqslant m \leqslant M$. The electric field of the pth eigenmode on the cross section S can thus be represented by a set of pulse basis functions as

$$\boldsymbol{E}_p(\boldsymbol{\rho}) = \sum_{\beta=x,y,z}\sum_{n=1}^{N}\sum_{m=1}^{M} a^{\beta}_{nm}\hat{\beta}P_n(x)R_m(z) \tag{10}$$

where

$$P_n(x) = \begin{cases}1, & x_n - D_x/2 \leqslant x \leqslant x_n + D_x/2 \\ 0, & \text{elsewhere}\end{cases}$$
$$R_m(z) = \begin{cases}1, & z_m - D_z/2 \leqslant z \leqslant z_m + D_z/2 \\ 0, & \text{elsewhere.}\end{cases} \tag{11}$$

Substituting (10) into (8), we have

$$\begin{aligned}&\sum_{\beta=x,y,z}\sum_{n=1}^{N}\sum_{m=1}^{M} a^{\beta}_{nm}\hat{\beta}P_n(x)R_m(z)\left[1 + \frac{\epsilon_{nm} - \epsilon_l}{\epsilon_l}\delta_{\beta z}\right] \\ &\quad = \frac{i}{4\pi}\omega^2\mu_0\sum_{\beta=x,y,z}\sum_{n=1}^{N}\sum_{m=1}^{M} a^{\beta}_{nm}(\epsilon_{nm} - \epsilon_l) \cdot \int\int_{S_{nm}} d\boldsymbol{\rho}' P_n(x')R_m(z') \\ &\quad\quad \cdot \int_{-\infty}^{\infty} dk_x e^{ik_x(x-x')}\bar{\bar{g}}_{ll}(k_x, \eta, z, z')\cdot\hat{\beta}, \qquad \boldsymbol{\rho} \text{ on } S\end{aligned} \tag{12}$$

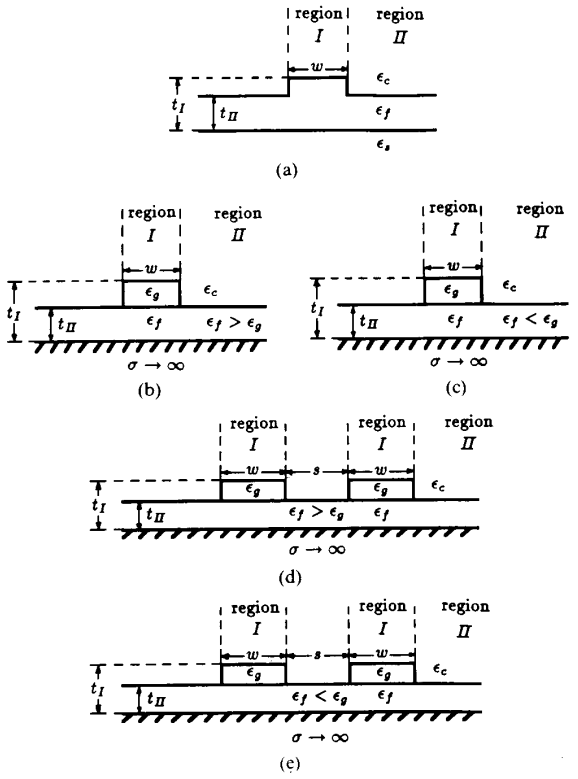

Fig. 2. The dielectric strip waveguides analyzed in this paper: (a) Optical rib waveguide. (b) Strip dielectric guide. (c) Insulated image guide. (d) Coupled strip dielectric guides. (e) Coupled insulated image guides.

where $\delta_{\alpha\beta}$ is the Kronecker delta function, which is equal to 1 when $\alpha=\beta$ and is equal to 0 when $\alpha\neq\beta$, and ϵ_{nm} is the dielectric constant evaluated at (x_n, z_m).

Next, we choose the same set of basis functions as the testing functions and apply Galerkin's method to (12). Taking the inner product of $\hat{\alpha}P_r(x)R_q(z)$ with (12), we obtain

$$\pi i\omega^2\mu_0 \sum_{\beta=x,y,z}\sum_{n=1}^{N}\sum_{m=1}^{M} a_{nm}^{\beta}(\epsilon_{nm}-\epsilon_l) \cdot\int_{-\infty}^{\infty} dk_x e^{ik_x(x_r-x_n)}\tilde{P}_r(-k_x)\tilde{P}_n(k_x)\hat{g}_{\alpha\beta}^{qm}(k_x,\eta) = A_{rq}\left[1+\frac{\epsilon_{rq}-\epsilon_l}{\epsilon_l}\delta_{\alpha z}\right]a_{rq}^{\alpha}. \quad (13)$$

Here $\alpha=x, y, z$; $1\leqslant r\leqslant N$ and $1\leqslant q\leqslant M$; A_{rq} is the area of S_{rq}; $\tilde{P}_n(k_x)$ is the Fourier transform of $P_n(x)$ with

$$\tilde{P}_n(k_x)=\frac{1}{2\pi}\int_{-D_x/2}^{D_x/2} dx e^{-ik_x x}P_n(x)=\frac{\sin(k_xD_x/2)}{\pi k_x} \quad (14)$$

and $\hat{g}_{\alpha\beta}^{qm}(k_x,\eta)$ is the $\alpha\beta$ component of the dyadic $\bar{\bar{g}}^{qm}(k_x,\eta)$ with

$$\bar{\bar{g}}^{qm}(k_x,\eta)=\int_{l_q} dz R_q(z)\int_{l_m} dz' R_m(z')\bar{\bar{g}}_{ll}(k_x,\eta,z,z') \quad (15)$$

where l_q is the domain of $R_q(z)$.

By utilizing the symmetry properties of $\tilde{P}_n(k_x)$ and $\hat{g}_{\alpha\beta}^{qm}(k_x,\eta)$ with respect to k_x, (13) can be further reduced to

$$2\pi i\omega^2\mu_0 \sum_{\beta=x,y,z}\sum_{n=1}^{N}\sum_{m=1}^{M} a_{nm}^{\beta}(\epsilon_{nm}-\epsilon_l) \cdot\int_0^{\infty} dk_x \tilde{P}_r(k_x)\tilde{P}_n(k_x)W_{rq,nm}^{\alpha\beta}(k_x,\eta) = \sum_{\beta=x,y,z}\sum_{n=1}^{N}\sum_{m=1}^{M}\delta_{\alpha\beta}\delta_{rn}\delta_{qm}A_{nm}\left[1+\frac{\epsilon_{nm}-\epsilon_l}{\epsilon_l}\delta_{\beta z}\right]a_{nm}^{\beta} \quad (16)$$

where

$$W_{rq,nm}^{\alpha\beta}(k_x,\eta)=\begin{cases}\cos k_x(x_r-x_n)\hat{g}_{\alpha\beta}^{qm}(k_x,\eta), & (\alpha,\beta)=(x,x),(y,y),\\ & (y,z),(z,y),(z,z)\\ i\sin k_x(x_r-x_n)\hat{g}_{\alpha\beta}^{qm}(k_x,\eta), & (\alpha,\beta)=(x,y),(x,z),\\ & (y,x),(z,x).\end{cases} \quad (17)$$

Equation (16) is a matrix equation of the form

$$\sum_{\beta=x,y,z}\sum_{n=1}^{N}\sum_{m=1}^{M} Z_{rq,nm}^{\alpha\beta}a_{nm}^{\beta}=0 \quad (18)$$

where $\alpha=x, y, z$; $1\leqslant r\leqslant N$; and $1\leqslant q\leqslant M$. The eigenvalue η can thus be obtained by setting the determinant of the Z matrix in (18) to zero. Hence we have

$$\det[Z(\omega,\eta)]=0. \quad (19)$$

To solve the integral equation (9) for two symmetrical dielectric strip waveguides, we choose the same set of pulse basis functions as in (11) to represent the electric field on the cross section S_1 as

$$\boldsymbol{E}_p(\rho)=\sum_{\beta=x,y,z}\sum_{n=1}^{N}\sum_{m=1}^{M} a_{nm}^{\beta}\hat{\beta}P_n(x)R_m(z), \quad \rho \text{ on } S_1. \quad (20)$$

By symmetry, the electric field on the cross section S_2 can be represented as

$$\boldsymbol{E}_p(\rho)=\sum_{\beta=x,y,z}\sum_{n=1}^{N}\sum_{m=1}^{M} I_{\xi}^{\beta}a_{nm}^{\beta}\hat{\beta}P_n(-x)R_m(z), \quad \rho \text{ on } S_2 \quad (21)$$

where the subscript ξ in I_{ξ}^{β} designates the even mode when $\xi=e$ and the odd mode when $\xi=o$. The definition of I_{ξ}^{β} is

$$I_{\xi}^{\beta}=\begin{cases}1, & (\xi,\beta)=(o,x),(e,y),(e,z)\\ -1, & (\xi,\beta)=(e,x),(o,y),(o,z).\end{cases} \quad (22)$$

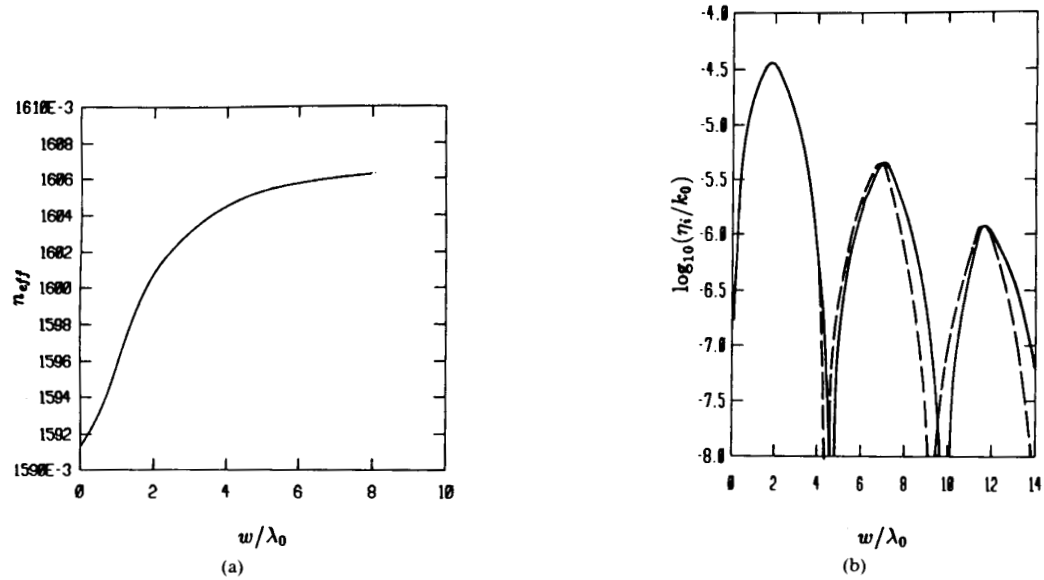

Fig. 3. The propagation constant for the E_{11}^z mode on the optical rib waveguide: $f = 30.0$ GHz, $t_1 = 0.8\lambda_0$, $t_{11} = 0.7\lambda_0$, $\epsilon_f = 2.8224\epsilon_0$, $\epsilon_s = 2.1904\epsilon_0$, $\epsilon_c = \epsilon_0$. (a) The real part; (b) the imaginary part: (a) — ours; ---- Ogusu's.

For an even (odd) mode, a magnetic (electric) wall can be put at $x = 0$ without affecting the field distributions.

Substituting (20) and (21) into (9) for ρ on S_1, we have

$$\sum_{\beta=x,y,z}\sum_{n=1}^{N}\sum_{m=1}^{M} a_{nm}^{\beta}\hat{\beta}P_n(x)R_m(z)\left[1+\frac{\epsilon_{nm}-\epsilon_l}{\epsilon_l}\delta_{\beta z}\right]$$
$$=\frac{i}{4\pi}\omega^2\mu_0\sum_{\beta=x,y,z}\sum_{n=1}^{N}\sum_{m=1}^{M} a_{nm}^{\beta}(\epsilon_{nm}-\epsilon_l)$$
$$\cdot\iint_{S_{nm}} d\rho'\left[P_n(x')+I_\xi^\beta P_n(-x')\right]R_m(z')$$
$$\cdot\int_{-\infty}^{\infty} dk_x e^{ik_x(x-x')}\bar{\bar{g}}_{ll}(k_x,\eta,z,z')\cdot\hat{\beta}, \qquad \rho \text{ on } S_1. \tag{23}$$

Due to the symmetry of the structure, only the electric fields on S_1 need to be tested when applying Galerkin's method. Taking the inner product of $\hat{\alpha}P_r(x)R_q(z)$ with (23) and utilizing the symmetry properties with respect to k_x, we have

$$2\pi i\omega^2\mu_0\sum_{\beta=x,y,z}\sum_{n=1}^{N}\sum_{m=1}^{M} a_{nm}^{\beta}(\epsilon_{nm}-\epsilon_l)$$
$$\cdot\int_0^{\infty} dk_x \tilde{P}_r(k_x)\tilde{P}_n(k_x)W_{rq,nm}^{\alpha\beta(\xi)}(k_x,\eta)$$
$$=\sum_{\beta=x,y,z}\sum_{n=1}^{N}\sum_{m=1}^{M}\delta_{\alpha\beta}\delta_{rn}\delta_{qm}A_{nm}\left[1+\frac{\epsilon_{nm}-\epsilon_l}{\epsilon_l}\delta_{\beta z}\right]a_{nm}^{\beta} \tag{24}$$

where $\alpha = x, y, z$; $1 \leqslant r \leqslant N$ and $1 \leqslant q \leqslant M$; and

$$W_{rq,nm}^{\alpha\beta(\xi)}(k_x,\eta)$$
$$=\begin{cases}\left[\cos k_x(x_r-x_n)+I_\xi^\beta\cos k_x(x_r+x_n)\right]\hat{g}_{\alpha\beta}^{qm}(k_x,\eta), \\ \quad(\alpha,\beta)=(x,x),(y,y),(y,z),(z,y),(z,z) \\ i\left[\sin k_x(x_r-x_n)+I_\xi^\beta\sin k_x(x_r+x_n)\right]\hat{g}_{\alpha\beta}^{qm}(k_x,\eta), \\ \quad(\alpha,\beta)=(x,y),(x,z),(y,x),(z,x).\end{cases} \tag{25}$$

Equation (24) is a matrix equation, and the eigenvalue η can be obtained by setting the determinant of the matrix to zero.

IV. Results and Discussions

In this section, three different dielectric strip waveguides are investigated. They are the optical rib waveguide, the strip dielectric guide, and the insulated image guide as shown in Fig. 2. The central region of each structure is denoted as region I, and the background region is denoted as region II.

In Fig. 3, we present the results for an optical rib waveguide. In this case, the rib portion in region I is chosen as the cross section of the strip which is embedded in the background medium of a slab waveguide. We divide the cross section of the strip into two segments along the z direction, and eight to 24 segments along the x direction depending on the width of the rib. Muller's method [17] is used to search for the roots of the determinantal equation (19) with the initial guess provided by the EDC method [8]. The CPU time spent to calculate the propagation

constant at each frequency is about 7 min on a DEC VAX station 3500.

The imaginary part of the propagation constant for the TM-like E_{11}^z mode is shown as a function of the rib width. The leakage and cancellation phenomena are observed and compared with those in [1]–[3]. The results calculated by using our method show good agreement with those obtained by the mode-matching technique [3]. Here the effective refractive index is defined as

$$n_{\text{eff}} = \frac{\eta_r}{k_0}$$

where η_r is the real part of the propagation constant η.

The wave modes of the dielectric waveguides are hybrid modes in nature. In our notation, they are called E_{pq}^x modes (TE-like) when the TE_z portion is larger than the TM_z portion and are called E_{pq}^z modes (TM-like) when the TE_z portion is less than the TM_z portion.

In Fig. 4(a), we present the effective refractive index n_{eff} for the E_{11}^x and E_{11}^z modes as a function of the thickness in region I of an optical rib waveguide with the rib width as parameter. The effective refractive indexes for the surface wave modes on region I and region II as if they were of infinite extent are also displayed in the figure.

The effective refractive index of the TE-like mode E_{11}^x is greater than that of the TM_0^{II} mode. Therefore, the k_x for the TM_0^{II} mode is imaginary because $k_x^2 = (n_i^2 - n_{\text{eff}}^2)k_0^2$; and no surface wave modes are excited to incur leakage. Here n_i is the effective refractive index of the TM_0^{II} mode. Meanwhile, the effective refractive index of the TM-like mode E_{11}^z is smaller than that of the TE_0^{II} mode for certain values of t_1. In that case, η is complex with a positive imaginary part, and k_x is complex with a negative imaginary part because the separation relation for the TE_0^{II} mode implies that $\eta_r\eta_i = -k_{xr}k_{xi}$. Here $\eta = \eta_r + i\eta_i$ and $k_x = k_{xr} + ik_{xi}$ with η_r, η_i, and k_{xr} positive. Usually, η_i is much less than η_r, and hence $|k_{xi}|$ is much less than k_{xr}.

The presence of the real part of k_x implies that the excited surface wave mode propagates away from the guiding strip with an exiting angle $\theta = \sin^{-1}(k_{xr}/(n_i k_0))$ with respect to the y axis, as was observed in [2].

The negative imaginary part of k_x implies that the magnitude of the exiting surface wave mode increases in the x direction. This phenomenon can be explained as follows: as the hybrid leaky mode is propagating along the y direction, surface waves are excited in the background medium, which propagate away from the guiding structure with an exiting angle θ. The magnitude of the hybrid mode decreases along the y direction due to leakage; hence the magnitude of the excited surface wave also decreases along the y direction. If we observe the field along the x direction ($y = \text{const}$), the surface wave at large value of x is excited from the propagating wave along the guide having larger magnitude than that which excites the surface wave at the small value of x.

To predict the occurrence of leakage, let us consider the case of $w = 2\lambda_0$ in Fig. 4. When the thickness t_1 is smaller than that at point T, the leakage occurs; when the thickness is larger than that at point T, the leakage vanishes. This figure not only indicates which modes leak and which do not; it also shows the range of geometrical and electrical parameters governing this phenomenon. Note that the leakage with $w = 6\lambda_0$ is smaller than that with $w = 2\lambda_0$ and larger than that with $w = 4\lambda_0$. This is consistent with the results in Fig. 3.

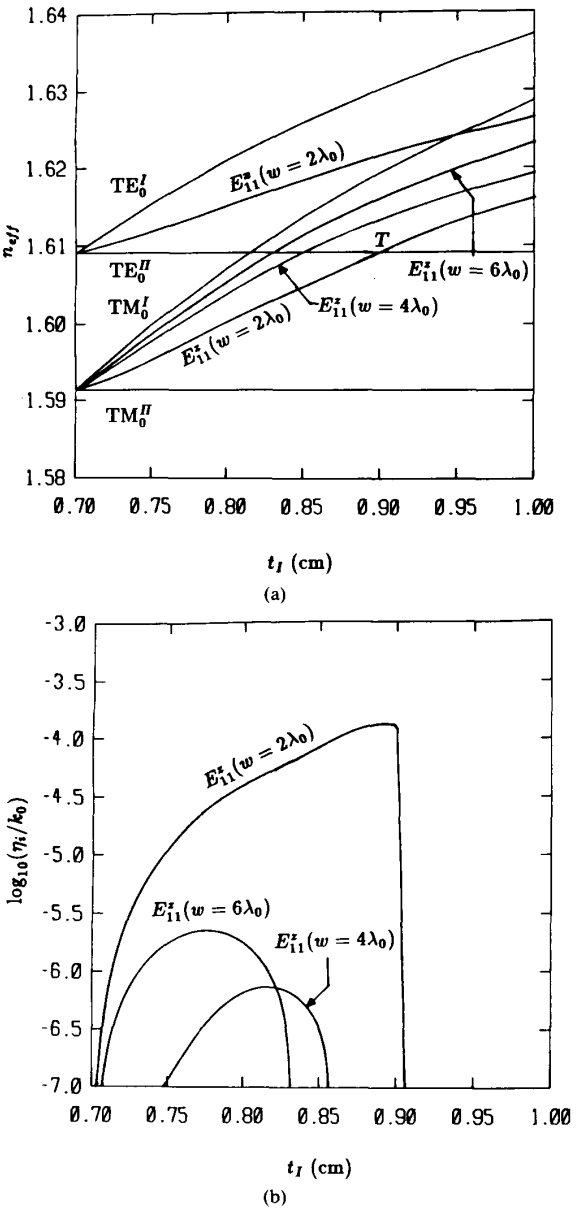

Fig. 4. (a) The effective refractive index for the modes on the optical rib waveguide: $f = 30.0$ GHz, $t_{\text{II}} = 0.7\lambda_0$, $\epsilon_f = 2.8224\epsilon_0$, $\epsilon_s = 2.1904\epsilon_0$, $\epsilon_c = \epsilon_0$. (b) The imaginary part of the propagation constant for the modes on the optical rib waveguide: $f = 30.0$ GHz, $t_{\text{II}} = 0.7\lambda_0$, $\epsilon_f = 2.8224\epsilon_0$, $\epsilon_s = 2.1904\epsilon_0$, $\epsilon_c = \epsilon_0$.

In Fig. 5, we present the propagation constants for the E_{11}^x and E_{11}^z modes on an insulated image guide. The effective refractive indexes of the surface wave modes on

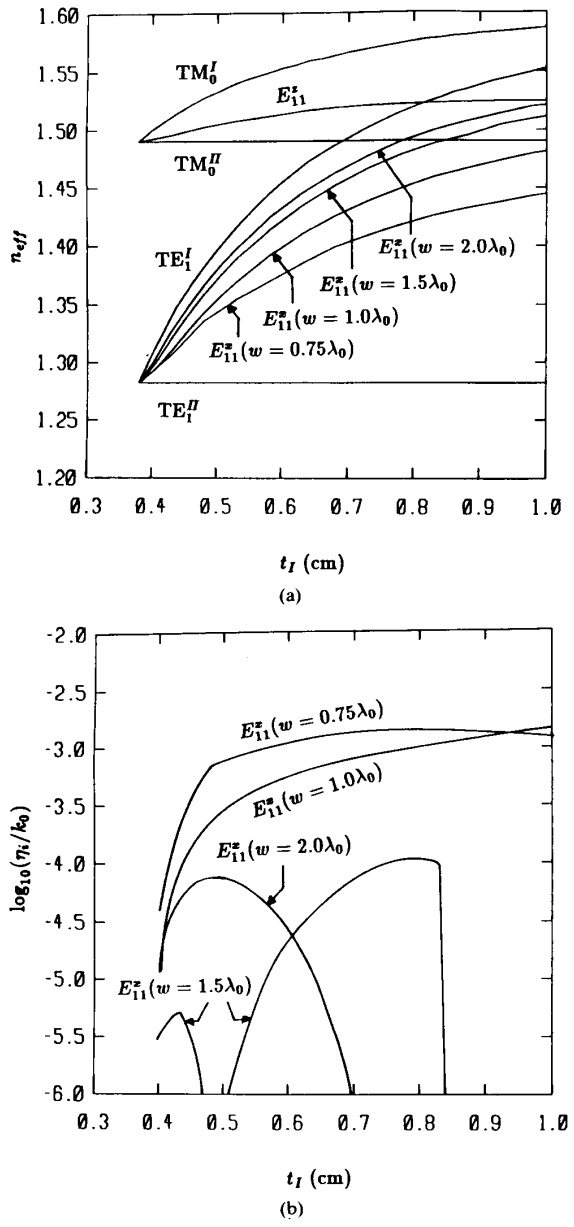

Fig. 5. (a) The effective refractive index for the modes on the insulated image guide: $f = 30.0$ GHz, $t_{II} = 0.38\lambda_0$, $\epsilon_g = 2.62\epsilon_0$, $\epsilon_f = 2.55\epsilon_0$, $\epsilon_c = \epsilon_0$. (b) The imaginary part of the propagation constant for the modes on the insulated image guide: $f = 30.0$ GHz, $t_{II} = 0.38\lambda_0$, $\epsilon_g = 2.62\epsilon_0$, $\epsilon_f = 2.55\epsilon_0$, $\epsilon_c = \epsilon_0$.

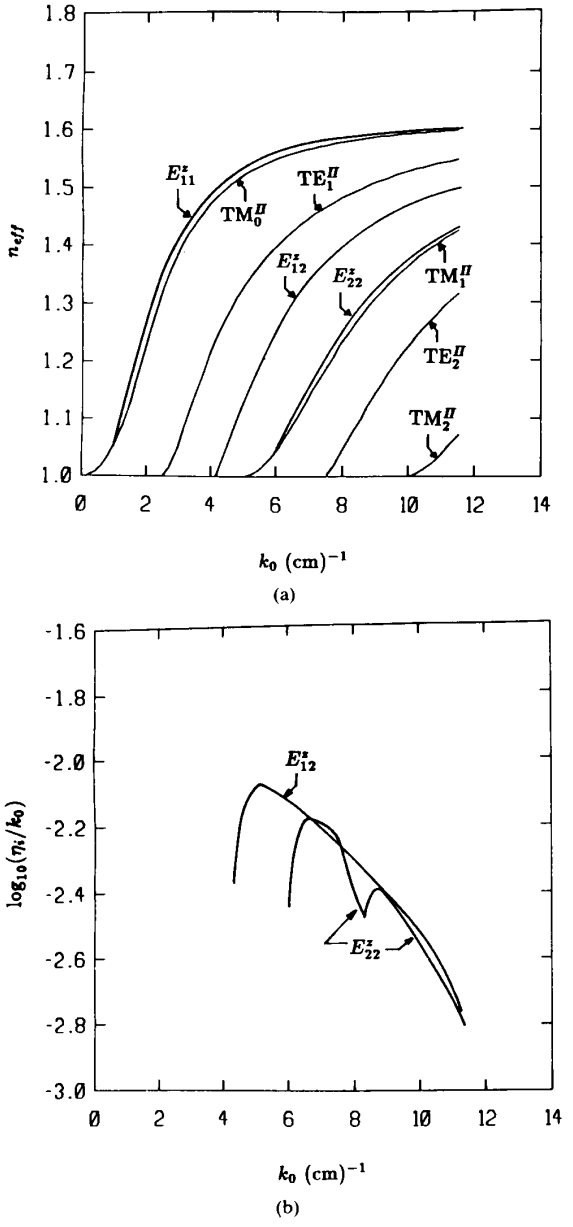

Fig. 6. (a) The effective refractive index for the TM-like modes on the strip dielectric guide: $t_I = 0.82$ cm, $t_{II} = 0.5$ cm, $w = 0.65$ cm, $\epsilon_g = 2.55\epsilon_0$, $\epsilon_f = 2.62\epsilon_0$, $\epsilon_c = \epsilon_0$. (b) The imaginary part of the propagation constant for the TM-like modes on the strip dielectric guide: $t_I = 0.82$ cm, $t_{II} = 0.5$ cm, $w = 0.65$ cm, $\epsilon_g = 2.55\epsilon_0$, $\epsilon_f = 2.62\epsilon_0$, $\epsilon_c = \epsilon_0$.

region I and region II are also displayed for reference. For the E_{11}^z mode, no surface waves are excited in region II. On the other hand, for the E_{11}^x mode, TM_0^{II} mode is excited to incur leakage.

From Figs. 4 and 5, it is clear that if the lowest order TE-like mode leaks, the lowest order TM-like mode does not leak; and vice versa.

In Fig. 6, we present the dispersion relation for three TM-like modes: E_{11}^z, E_{12}^z, and E_{22}^z on a strip dielectric guide. The dispersion relations of the first five slab waveguide modes on region II are also displayed for reference. The effective refractive index of the E_{11}^z mode is larger than that of any slab waveguide mode; hence no leakage is expected. For the E_{12}^z and the E_{22}^z modes, both the TM_0^{II} and TE_1^{II} surface wave modes are excited, and leakage is observed as the imaginary part of the propagation constant shown in Fig. 6(b).

In Fig. 7, we present the dispersion relation for two TE-like modes: the E_{11}^x and the E_{12}^x modes on a strip dielectric guide. The dispersion relations of the first five

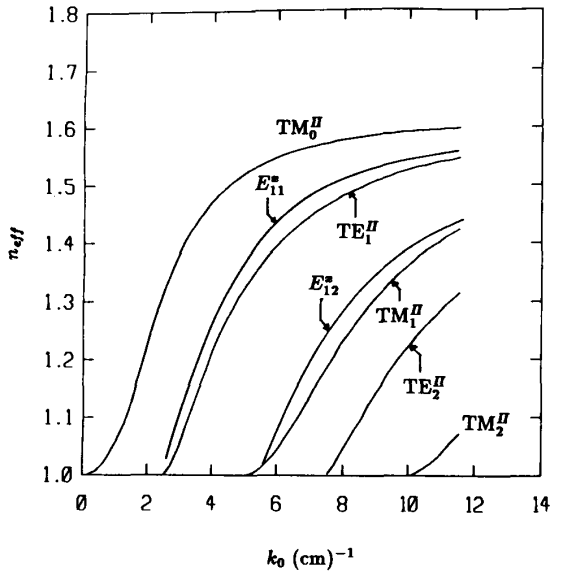

(a)

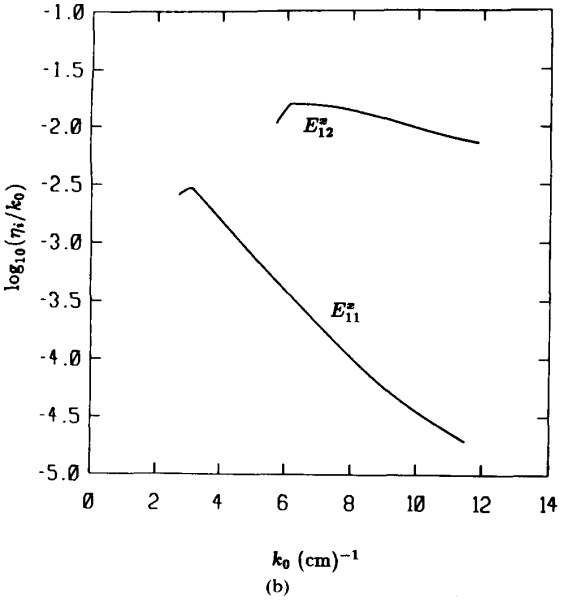

(b)

Fig. 7. (a) The effective refractive index for the TE-like modes on the strip dielectric guide: $t_I = 0.82$ cm, $t_{II} = 0.5$ cm, $w = 0.65$ cm, $\epsilon_g = 2.55\epsilon_0$, $\epsilon_f = 2.62\epsilon_0$, $\epsilon_c = \epsilon_0$. (b) The imaginary part of the propagation constant for the TE-like modes on the strip dielectric guide: $t_I = 0.82$ cm, $t_{II} = 0.5$ cm, $w = 0.65$ cm, $\epsilon_g = 2.55\epsilon_0$, $\epsilon_f = 2.62\epsilon_0$, $\epsilon_c = \epsilon_0$.

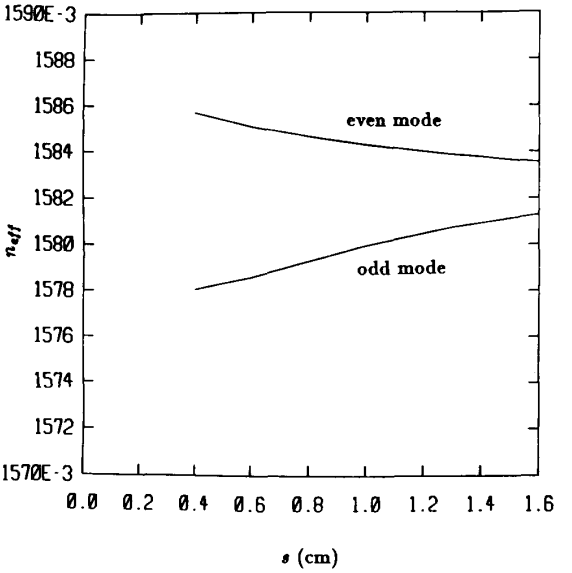

Fig. 8. The effective refractive index for the E_{11}^z modes on two identical strip dielectric guides: $f = 38.67$ GHz, $t_I = 0.82$ cm, $t_{II} = 0.5$ cm, $w = 0.65$ cm, $\epsilon_g = 2.55\epsilon_0$, $\epsilon_f = 2.62\epsilon_0$, $\epsilon_c = \epsilon_0$.

slab waveguide modes on region II are also displayed for reference. The effective refractive index of the E_{11}^x mode is smaller than that of the TM_0^{II} mode; hence the E_{11}^x mode is a leaky mode. For the E_{12}^x mode, both the TM_0^{II} and the TE_1^{II} mode are excited, and leakage is observed as the imaginary part of the propagation constant shown in Fig. 7(b). Thus, the E_{11}^x mode couples to the TM_0^{II} mode, which has an opposite polarization as was observed by Peng and Oilner [1], [2]. On the other hand, the E_{12}^z, the E_{22}^z, and the E_{12}^x mode couple to both the TM_0^{II} and the TE_1^{II} mode in the background medium. Hence, as the lowest order leaky mode couples to the surface wave mode of opposite polarization, the higher order leaky modes may couple to the surface wave modes of both polarizations. This was also observed by Ogusu [3]. The same conclusions can also be drawn for the insulated image guide.

From Figs. 6 and 7, it is observed that the E_{11}^z is a nonleaky mode, but the E_{11}^x is a leaky mode. This verifies the conclusions we drew from Figs. 4 and 5 that if the lowest TE-like (TM-like) mode is leaky, the lowest TM-like (TE-like) mode is nonleaky.

Next, we consider the coupling of two symmetrical dielectric strip waveguides. In Fig. 8, we show the effective refractive index of the E_{11}^z mode for two identical strip dielectric guides as a function of separation s. The effective refractive index of the even and odd modes tends to be degenerate as the separation increases, and no leakage is observed. Since the separation is large, the field distribution on each strip is the same as if the other strip were absent. For the corresponding single-strip case shown in Fig. 6, the E_{11}^z mode is a nonleaky mode, which implies that no surface wave modes are excited in the background region. As the separation is reduced, there are still no surface wave modes excited.

In Fig. 9, we present the propagation constant of the E_{11}^x mode for two symmetrical strip dielectric guides. The E_{11}^x mode on the corresponding single-strip dielectric guide is a leaky mode, as shown in Fig. 7. The effective refractive index of the even and odd modes tends to be degenerate as the separation increases, but a small oscillatory behavior is observed when the separation s is larger than 2.6 cm. As for the imaginary part of the propagation constant, when

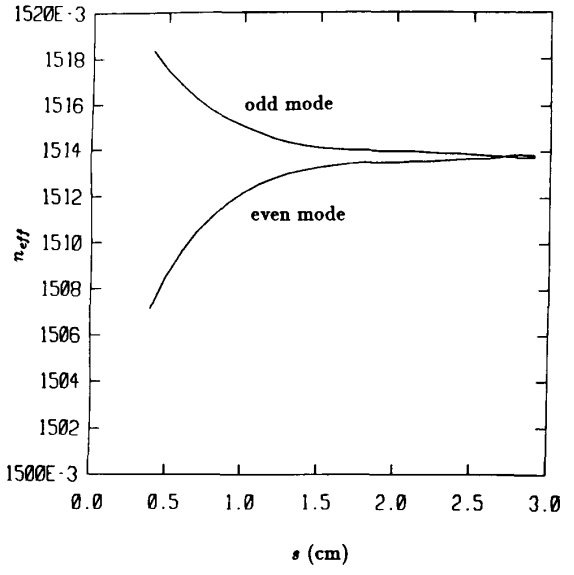

(a)

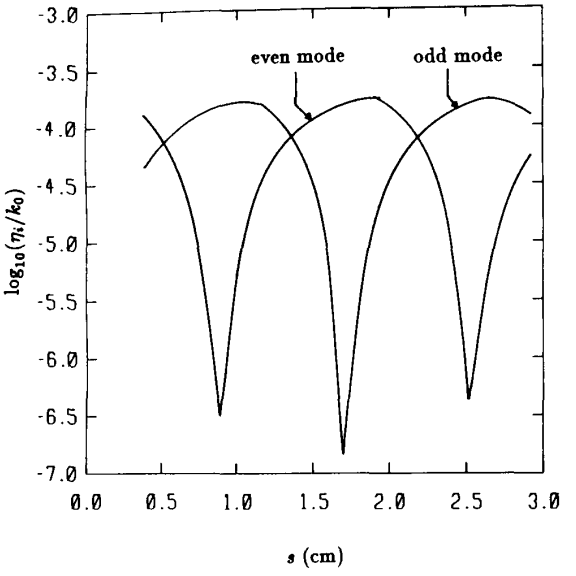

(b)

Fig. 9. (a) The effective refractive index for the E_{11}^{x} modes on two identical strip dielectric guides: $f = 40.0$ GHz, $t_{\mathrm{I}} = 0.82$ cm, $t_{\mathrm{II}} = 0.5$ cm, $w = 0.65$ cm, $\epsilon_g = 2.55\epsilon_0$, $\epsilon_f = 2.62\epsilon_0$, $\epsilon_c = \epsilon_0$. (b) The imaginary part of the propagation constant for the E_{11}^{x} modes on two identical strip dielectric guides: $f = 40.0$ GHz, $t_{\mathrm{I}} = 0.82$ cm, $t_{\mathrm{II}} = 0.5$ cm, $w = 0.65$ cm, $\epsilon_g = 2.55\epsilon_0$, $\epsilon_f = 2.62\epsilon_0$, $\epsilon_c = \epsilon_0$.

the even mode has a maximum, the odd mode has a null; and vice versa.

In Fig. 10, the propagation constant of the E_{12}^{z} mode is presented. The effective refractive index of both the even and the odd mode displays an oscillatory behavior. Where the even mode has a maximum, the odd mode has a minimum; the vice versa.

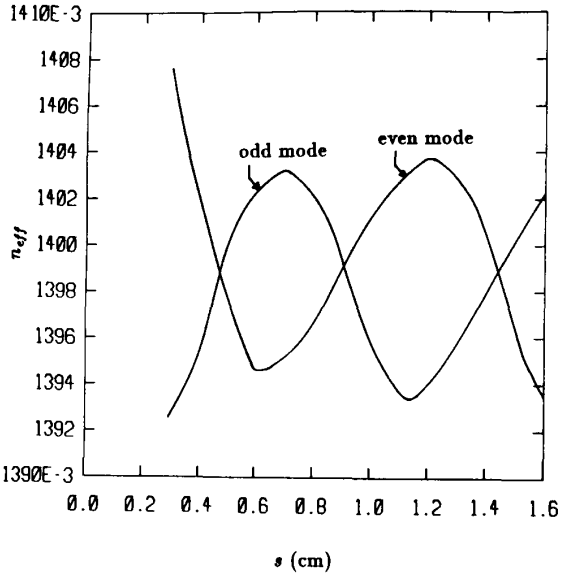

(a)

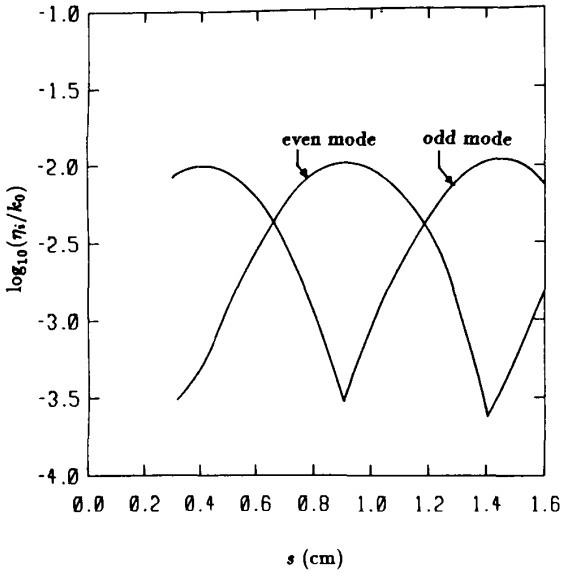

(b)

Fig. 10. (a) The effective refractive index for the E_{12}^{z} modes on two identical strip dielectric guides: $f = 38.67$ GHz, $t_{\mathrm{I}} = 0.82$ cm, $t_{\mathrm{II}} = 0.5$ cm, $w = 0.65$ cm, $\epsilon_g = 2.55\epsilon_0$, $\epsilon_f = 2.62\epsilon_0$, $\epsilon_c = \epsilon_0$. (b) The imaginary part of the propagation constant for the E_{12}^{z} modes on two identical strip dielectric guides: $f = 38.67$ GHz, $t_{\mathrm{I}} = 0.82$ cm, $t_{\mathrm{II}} = 0.5$ cm, $w = 0.65$ cm, $\epsilon_g = 2.55\epsilon_0$, $\epsilon_f = 2.62\epsilon_c = \epsilon_0$.

This behavior can be qualitatively explained by the following approximate formula for the propagation constants derived from the coupled wave equations [18]:

$$\eta_{\pm} = \eta \pm \Delta\eta, \qquad \Delta\eta = -\frac{\omega\epsilon_0}{4P}\iint_{S_1} d\rho\, \delta\epsilon(\rho)\boldsymbol{E}_1^{*}\cdot\boldsymbol{E}_2$$

where η is the propagation constant of the wave mode in the absence of the other waveguide; $\eta_{\pm}$ are the propaga-

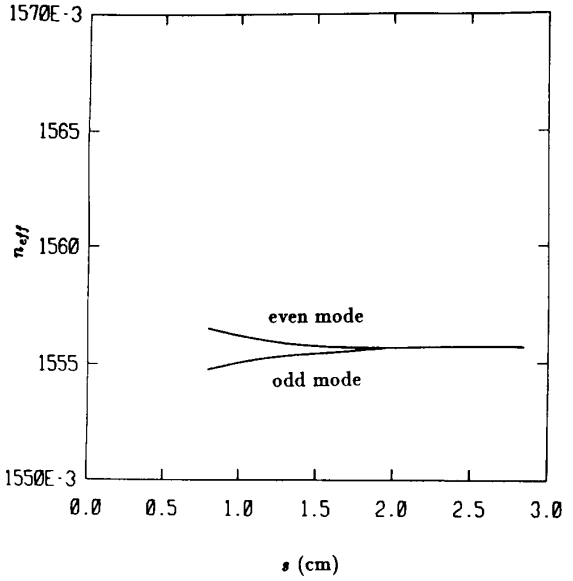

Fig. 11. The effective refractive index for the E_{11}^z modes on two identical insulated image guides: $f = 30.23$ GHz, $t_I = 0.83$ cm, $t_{II} = 0.38$ cm, $w = 1.5$ cm, $\epsilon_g = 2.62\epsilon_0$, $\epsilon_f = 2.55\epsilon_0$, $\epsilon_c = \epsilon_0$.

tion constants of the coupled modes when the two waveguides are both present; $\boldsymbol{E}_i$ is the electric field due to waveguide i in the absence of the other guide, where $i = 1, 2$; and P is the power guided by waveguide 1 alone.

For the nonleaky modes, the electric fields decay away from the central regions. Hence the overlapping integral decreases as the separation increases. For the leaky modes, the electric fields outside of the central regions are the superposition of an evanescent wave and the propagating surface waves. If the propagating wave portion is strong enough, it will make the overlapping integral change sign when the separation is changed; and the overlapping integral sustains even at large separation.

For two symmetrical dielectric strip guides, the overall leakage is due to the excitation of the surface wave modes in the background medium by both guides. At certain separation when the even mode has a maximum leakage, it implies that the surface wave modes excited by each waveguide add in phase. For the odd mode at the same separation, these surface wave modes add out of phase due to the definition of the even and odd modes; hence the cancellation effect is observed as a null in the imaginary part of the propagation constant. Similarly, if the odd mode has a maximum leakage at a certain separation, the even mode shows a cancellation effect.

The small oscillation in Fig. 9(a), however, does not contradict the aforementioned explanation because the leakage loss is almost two orders smaller than that of the E_{12}^z mode; hence the contribution of the propagating surface wave to the overlapping integral is negligibly small.

In Fig. 11, we show the effective refractive index for the E_{11}^z modes on two identical insulated image guides. The

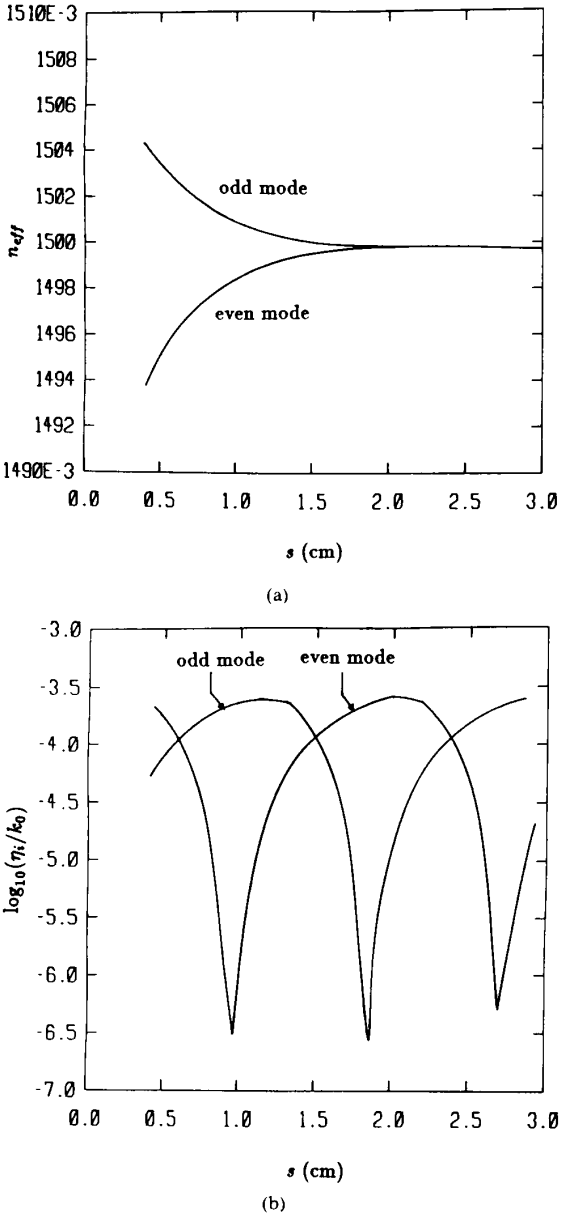

Fig. 12. (a) The effective refractive index for the E_{11}^x modes on two identical insulated image guides: $f = 40.0$ GHz, $t_I = 0.82$ cm, $t_{II} = 0.5$ cm, $w = 0.65$ cm, $\epsilon_g = 2.62\epsilon_0$, $\epsilon_f = 2.55\epsilon_0$, $\epsilon_c = \epsilon_0$. (b) The imaginary part of the propagation constant for the E_{11}^x modes on two identical insulated image guides: $f = 40.0$ GHz, $t_I = 0.82$ cm, $t_{II} = 0.5$ cm, $w = 0.65$ cm, $\epsilon_g = 2.62\epsilon_0$, $\epsilon_f = 2.55\epsilon_0$, $\epsilon_c = \epsilon_0$.

even and odd modes tend to be degenerate when the separation is increased. The E_{11}^z modes are nonleaky modes as the corresponding E_{11}^z mode on the single insulated image guide. In Fig. 12, we show the propagation constant of the E_{11}^x modes on two identical insulated image guides. The effective refractive index of the even and odd modes tends to be degenerate, and the imaginary part displays maxima and nulls alternatively.

V. Conclusions

The guidance and leakage properties of single and coupled dielectric strip waveguides are analyzed using a dyadic Green's function and integral equation formulation. Galerkin's method is used to solve the integral equation for the dispersion relation. A method to predict the occurrence of leakage is proposed. The leakage occurs when the effective refractive index is smaller than those of the surface wave modes in the background medium. For the coupled dielectric strip waveguides, the dispersion relations of the even and odd leaky modes are investigated.

References

[1] S. T. Peng and A. A. Oliner, "Guidance and leakage properties of a class of open dielectric waveguides: Part I—Mathematical formulations," *IEEE Trans. Microwave Theory Tech.*, vol. MTT-29, pp. 843–855, Sept. 1981.

[2] A. A. Oliner, S. T. Peng, T. I. Hsu, and A. Sanchez, "Guidance and leakage properties of a class of open dielectric waveguides: Part II —New physical effects," *IEEE Trans. Microwave Theory Tech.*, vol. MTT-29, pp. 855–869, Sept. 1981.

[3] K. Ogusu, "Optical strip waveguide: A detailed analysis including leaky modes," *J. Opt. Soc. Amer.*, vol. 73, no. 3, pp. 353–357, Mar. 1983.

[4] K.Ogusu, S. Kawakami, and S. Nishida, "Optical strip waveguide: An analysis," *Appl. Opt.*, vol. 18, no. 6, pp. 908–914, Mar. 1979.

[5] K. Ogusu, S. Kawakami, and S. Nishida, "Optical strip waveguide: An analysis: a correction," *Appl. Opt.*, vol. 18, no. 22, p. 3725, Nov. 1979.

[6] K. Ogusu and I. Tanaka, "Optical strip waveguide: An experiment," *Appl. Opt.*, vol. 19, no. 19, pp. 3322–3325, Oct. 1980.

[7] E. A. J. Marcatili, "Dielectric rectangular waveguide and directional coupler for integrated optics," *Bell Syst. Tech. J.*, vol. 48, pp. 2071–2102, Sept. 1969.

[8] W. V. McLevige, T. Itoh, and R. Mittra, "New waveguide structures for millimeter-wave and optical integrated circuits," *IEEE Trans. Microwave Theory Tech.*, vol. MTT-23, pp. 788–794, Oct. 1975.

[9] R. Mittra, Y. L. Hou, and V. Jamnejad, "Analysis of open dielectric waveguides using mode-matching technique and variational methods," *IEEE Trans. Microwave Theory Tech.*, vol. MTT-28, pp. 36–43, Jan. 1980.

[10] M. Tsuji, S. Suhara, H. Shigesawa, and K. Taiyama, "Submillimeter guided-wave experiments with dielectric rib waveguides," *IEEE Trans. Microwave Theory Tech.*, vol. MTT-29, pp. 547–552, June 1981.

[11] K. Hayata, M. Koshiba, M. Eguchi, and M. Suzuki, "Vectorial finite-element method without any spurious solutions for dielectric waveguiding problems using transverse magnetic-field component," *IEEE Trans. Microwave Theory Tech.*, vol. MTT-34,pp. 1120–1124, Nov. 1986.

[12] K. Hayata, M. Eguchi, and M. Koshiba, "Self-consistent finite/infinite element scheme for unbounded guided wave problems," *IEEE Trans. Microwave Theory Tech.*, vol. 36, pp. 614–616, Mar. 1988.

[13] K. Bierwirth, N. Schulz, and F. Arndt, "Finite-difference analysis of rectangular dielectric waveguide structures," *IEEE Trans. Microwave Theory Tech.*, vol. MTT-34, pp. 1104–1114, Nov. 1986.

[14] J. S. Bagby, D. P. Nyquist, and B. C. Drachman, "Integral formulation for analysis of integrated dielectric waveguides," *IEEE Trans. Microwave Theory Tech.*, vol. MTT-33, pp. 906–915, Oct. 1985.

[15] J. A. Kong, *Electromagnetic Wave Theory*. New York: Wiley, 1986.

[16] S. M. Ali, T. M. Habashy, and J. A. Kong, "Dyadic Green's functions for multilayered uniaxially anisotropic media," *J. Electromagn. Waves Appl.*, submitted for publication.

[17] A. Ralston, *A First Course in Numerical Analysis*. New York: McGraw-Hill, 1965.

[18] D. Marcuse, *Light Transmission Optics*. New York: Van Nostrand Reinhold, 1972.

Jean-Fu Kiang was born in Taipei, Taiwan, R.O.C., and February 2, 1957. He received the B.S. and M.S. degrees in electrical engineering from National Taiwan University in 1979 and 1981, respectively. In 1983, he became a research and teaching assistant in the Department of Electrical Engineering and Computer Science at M.I.T., where he obtained the M.S. and Ph.D. degrees in 1985 and March 1989, respectively.

Since then, he has been working at IBM Research, Yorktown Heights, N.Y. His research interests are electromagnetic theory and applications and numerical analysis.

Dr. Kiang is a member of Sigma Xi.

Sami M. Ali (M'79–SM'86) was born in Egypt on December 7, 1938. He received the B.S. degree from the Military Technical College, Cairo, Egypt, in 1965, and the Ph.D. degree from the Technical University of Prague, Prague, Czechoslovakia, in 1975, both in electrical engineering.

He joined the Electrical Engineering Department, Military Technical College, Cairo, in 1975. In 1985, he became a Professor and head of the Basic Electrical Engineering Department there. From 1981 to 1982 he was a visiting scientist at the Research Laboratory of Electronics, M.I.T. Cambridge, MA. Since 1987, he has again been a visiting scientist there. His current research interests deal with microwave integrated circuits and microstrip antenna applications.

Jin Au Kong is Professor of Electrical Engineering and Chairman of Area IV and Energy and Electromagnetic Systems in the Department of Electrical Engineering and Computer Science at the Massachusetts Institute of Technology in Cambridge, Massachusetts. From 1977 to 1980 he served the United Nations as a High-Level Consultant to the Under-Secretary-General on science and technology, and as an Interregional Advisor on remote sensing technology for the Department of Technical Cooperation for Development. His research interest is in the area of electromagnetic wave theory and applications.

Dr. Kong is the Editor for the Wiley series on remote sensing, the Editor-in-Chief of the *Journal of Electromagnetic Waves and Applications* (*JEWA*), and the Chief Editor for the Elsevier book series on Progress in Electromagnetics Research (PIER).